(Ce, Gd):YAG-Al2O3 composite ceramics for high-brightness yellow light-emitting diode applications

Xiaoyun Li
FIRSM: Chinese Academy of Sciences Fujian Institute of Research on the Structure of Matter
Jian Chen
FIRSM: Chinese Academy of Sciences Fujian Institute of Research on the Structure of Matter
https://orcid.org/0000-0001-6091-614X
Zhuguang Liu
FIRSM: Chinese Academy of Sciences Fujian Institute of Research on the Structure of Matter
Zhonghua Deng
FIRSM: Chinese Academy of Sciences Fujian Institute of Research on the Structure of Matter
Qiufeng Huang
FIRSM: Chinese Academy of Sciences Fujian Institute of Research on the Structure of Matter
Jiquan Huang
FIRSM: Chinese Academy of Sciences Fujian Institute of Research on the Structure of Matter
Wang Guo (guowang@fjirsm.ac.cn)
FIRSM: Chinese Academy of Sciences Fujian Institute of Research on the Structure of Matter

Research Article

Keywords: (Ce,Gd):YAG-Al2O3, composite ceramics, yellow LEDs, thermal conductivity, operating temperature

Posted Date: August 24th, 2021

DOI: https://doi.org/10.21203/rs.3.rs-829168/v1

Version of Record: A version of this preprint was published at Journal of the European Ceramic Society on November 1st, 2021. See the published version at
https://doi.org/10.1016/j.jeurceramsoc.2021.11.027.

(Ce, Gd):YAG-Al_2O_3 composite ceramics for high-brightness yellow light-emitting diode applications

Xiaoyun LI[a,b], Jian CHEN[a,c,*], Zhuguang LIU[a,c], Zhonghua DENG[a,c], Qiufeng HUANG[a,c], Jiquan HUANG[a,c], Wang GUO[a,c,*]

[a]*Key Laboratory of Optoelectronic Materials Chemistry and Physics, Fujian Institute of Research on the Structure of Matter, Chinese Academy of Sciences, Fuzhou, 350002, P. R. China*

[b]*College of Chemistry and Materials Science, Fujian Normal University, Fuzhou 350002, China*

[c]*Fujian Science & Technology Innovation Laboratory for Optoelectronic Information of China, Fuzhou, Fujian 350108, P. R. China*

**Corresponding author. E-mail: guowang@fjirsm.ac.cn; chenjian@fjirsm.ac.cn*

Abstract

Gd^{3+} ions were doped in Ce:YAG ceramics as the phosphor material for the high-brightness yellow LED (565-590 nm). Besides the role of spectral modulation, the introduction of Gd^{3+} ions also exacerbates the thermal quenching effect. To increase its thermal performance, Al_2O_3 were introduced as the second phase and $(Ce_{0.6\%}Y_{69.4\%}Gd_{30\%})_3Al_5O_{12}$-z% Al_2O_3 (z=0, 10, 20, 30, 40) composite ceramics were fabricated by vacuum sintering. Their composite microstructures and phase structures were characterized. As the amount of Al_2O_3 increases from 0 wt% to 40 wt%, there is a noticeable improvement on the thermal conductivity. The thermal stability also increases and the operating temperature of ceramics reduced from 141.1 °C to 132.2 °C. Collaborating composite ceramics with InGaN blue chips, the steady-state luminous efficiency of 40 wt%-Al_2O_3 yellow LED reaches the highest value of 109.49 lm/W, which is 8.54 % higher than that of Al_2O_3-free sample. Additionally, scattering behavior and conversion efficiency of composite ceramics with different thicknesses were investigated.

Keywords

(Ce,Gd):YAG-Al_2O_3; composite ceramics; yellow LEDs; thermal conductivity; operating temperature

1. Introduction

Solid-state lighting (SSL), particularly light-emitting diode (LED) based SSL, is on course to become the dominant technology across all lighting applications.[1-4] Among monochromatic LEDs, high-brightness yellow LED (565-590 nm) has excellent penetration performance and is close to the sensitive wavelength of human eyes, which has extensive applications in fog lamp, underwater lighting, stage lighting, etc. To date, direct-emitting yellow LED are still inefficient. The power conversion of yellow LED is lower than 20 %, while that of blue LED reaches about 70 %.[5, 6]

To produce high-efficiency yellow light, the phosphor-converted LED architecture proves to be the most effective for now.[7] Ce^{3+} ions are doped in $Y_3Al_5O_{12}$ (YAG) as

the luminescent ions, attributed to 4f-5d transition of Ce^{3+} ions. Its high quantum efficiency and thermal stability has been verified in white LED applications.[8-10] Excited by 450 nm blue light, the excited electrons in the lowest of 5d energy level of Ce^{3+} ions in YAG decay to the ground state and then emit yellowish green light with a central wavelength of 530-550 nm. In order to realize the yellow LED (565-590 nm), larger Gd^{3+} ions can be doped to partially replace smaller Y^{3+} ions for the red shift of emission spectrum, attributed to the enhancement of crystal field by lattice expansion.[11-13] However, by the introduction of Gd^{3+} ions, the lowest 5d energy level of Ce^{3+} gets lower and consequently the activation energy (ΔE) of thermally induced non-radiative transition decreases.[14-16] Thus, the luminous efficiency of yellow LED based on (Ce,Gd):YAG phosphor drops faster than that of samples without Gd^{3+} ions as temperature increases. Thermal stability and thermal quenching behavior become the core issue in research on Gd-based yellow LED.

Therefore, for high-brightness yellow light-emitting diode applications, the doping concentration of Ce^{3+} and Gd^{3+} should be first studied by the corresponding electroluminescent spectra. Then more attention should be paid to the thermal-optical performance of phosphor-converted yellow LED. Phosphor materials with high thermal conductivity are required for the heat dissipation of high-brightness yellow LED. (Ce, Gd):YAG-Al_2O_3 composite ceramic is one of the most suitable candidates of phosphor materials, due to the high thermal conductivity of Al_2O_3 (32-35 W m^{-1} K^{-1}), which has been applied in high-power-density laser illumination in recent years.[17-20] Moreover, Al_2O_3 phase has no absorption in the visible region and won't react with YAG, thus ensuring that Al_2O_3 won't cause interference to the luminescent properties of (Ce,Gd):YAG. Besides, light can be scattered in (Ce, Gd):YAG-Al_2O_3 composite ceramics due to the different refractive indexes between YAG and Al_2O_3 phase and consequently increases the extraction efficiency. The thermal conductivity of composite ceramics, thermal quenching behavior, light scattering performance, and luminescent properties of ceramic-based yellow LEDs (CB-yLEDs) are highly related to the mixture ratio of composite ceramics, which needs to be studied systematically.

In this paper, two series of $(Ce_{0.6\%}Y_{99.4\%-x\%}Gd_{x\%})_3Al_5O_{12}$ (x = 0, 10, 20, 30, 40, 50) and $(Ce_{y\%}Y_{70\%-y\%}Gd_{30\%})_3Al_5O_{12}$ (y = 0.4, 0.5, 0.6, 0.7) transparent ceramics were prepared by vacuum sintering technology. According to their spectra and luminescent properties of ceramics-based LEDs, $(Ce_{0.6\%}Y_{69.4\%}Gd_{30\%})_3Al_5O_{12}$ was selected as the luminescent material. Then, $(Ce_{0.6\%}Y_{69.4\%}Gd_{30\%})_3Al_5O_{12}$-z% Al_2O_3 (z = 0, 10, 20, 30, 40) composite ceramics with different Al_2O_3 amount were prepared. Their composite structures were characterized by X-ray diffractions and scanning electron microscopy. The thermal conductivity and temperature dependent emission spectra of composite ceramics were recorded. Encapsulated on blue chips and excited by 450 nm LED excitation, relationships between composite proportion, operating temperature and luminescent properties of CB-yLEDs were studied. Besides, the scattering behavior and conversion efficiency of composite ceramics with different thicknesses were revealed.

2. Experimental section

2.1 Material fabrication

$(Ce_{0.6\%}Y_{99.4\%-x\%}Gd_{x\%})_3Al_5O_{12}$ (x = 0~50), $(Ce_{y\%}Y_{70\%-y\%}Gd_{30\%})_3Al_5O_{12}$ (y = 0.4~0.7), and $(Ce_{0.6\%}Y_{69.4\%}Gd_{30\%})_3Al_5O_{12}$-z% Al_2O_3 (z = 0~40) ceramics were fabricated by solid-state reactive sintering approach. High-pure α-Al_2O_3 (99.99%, Sumitomo Chemical Co. Ltd, Japan), Y_2O_3, CeO_2, and Gd_2O_3 (99.99%, Alfa Aesar) were employed as the precursor material. Stoichiometric amounts of raw materials were ground in planetary-milling machine for 24 h. The mixed powders were pressed into Φ20 mm and Φ35 mm disks. After de-bindered at 800 °C in oxygen, the green compacts were pressed by the cold isostatic presses at 196 MPa. Then, they were sintered under vacuum condition at 1730 °C for 8 h. It is noteworthy that the annealing temperature was set at 1000 °C, according to the results of our previous works.[21]

2.2 Properties characterization

X-ray diffraction was carried out using Cu Kα radiation with a scan step width of 0.02° (Mini Flex600, Rigaku, Japan). The in-line transmittance of composite ceramics was obtained by using an UV/Vis/NIR spectrophotometer (Lambda-900, PerkinElmer, USA). Decay curves and the temperature dependence of photoluminescence (PL) and were recorded with a spectrometer (FLS1000, Edinburgh instrument, United Kingdom). The morphology observations were performed through a JSM-6700F field emission scanning electron microscope (FE-SEM, JEOL, Japan). The thermal conductivity was measured by a laser flash apparatus (LFA467, Netzsch, Germany).

Six 1.4×1.4 mm InGaN/GaN LED chips were mounted on aluminum nitride substrate, and then covered them with the ceramic samples, which severs as light converter. 0.2 mm-thickness composite ceramics were cut into square slice (1.4×1.4 mm), and then packaged on these six chips. The chips were spaced regularly, about 100 μm apart and the size of emitting area was about 4.4×2.9 mm. Time dependence of temperature of composite ceramics (T_c) and substrate (T_s) at runtime were monitored by thermal imaging camera system (Flir A300, America). Optical properties of CB-yLEDs such as correlative color temperature (CCT), luminous flux (LF), luminous efficiency (LE), and Commission International de l'Éclairage (CIE) coordinates were tested by using the integrated optical and electrical measuring system (Everfine, Hangzhou). The forward current of the blue chips were fixed at 1.3 A.

3. Results and discussion

3.1 Preparation of (Ce,Gd):YAG ceramics

$(Ce_{0.6\%}Y_{99.4\%-x\%}Gd_{x\%})_3Al_5O_{12}$ (x=0, 10, 20, 30, 40, 50) transparent ceramics were prepared to investigate the relationship between the emission spectrum and Gd^{3+}

concentrations. XRD patterns of 0.6 at% Ce:YAG transparent ceramics with different concentration of Gd^{3+} ions are shown in Fig. 1a. All diffraction peaks match well with those of cubic $Y_3Al_5O_{12}$ phase (JCPDS No. 79-1892). Note that positions of diffraction peaks gradually move to lower angle as Gd^{3+} concentration increases from 0 at% to 50 at%, mainly due to the lattice expansion by the substitution of Y^{3+} ions (1.019 Å, coordination = 8) with larger Gd^{3+} ions (1.053 Å, coordination = 8). The lattice expansion also results in the enhancement of crystal field and therefore red shift of Ce^{3+} emission spectrum from 548 nm to 579 nm (Fig. 1b). The corresponding colors of Ce:YAG ceramics change from yellowish green to orange, as shown in Fig. 1b.

The InGaN/GaN LED chips were mounted on aluminum nitride substrate, and then covered them with ceramics. Their emission spectrum, CCT, and CIE color coordinates of CB-yLEDs are tabulated in table 1. When the doping concentration of Gd^{3+} ions reaches 30 at%, the corresponding LED emits yellow light with the central emission wavelength of 568 nm, which is suitable for the yellow LED applications.

In consideration of the heat dissipation and secondary light distribution on optical encapsulated structure of LED, the thickness of phosphor ceramics is usually less than 200 μm. So we designed another series of $(Ce_{y\%}Y_{70\%-y\%}Gd_{30\%})_3Al_5O_{12}$ (y=0.4, 0.5, 0.6, 0.7) transparent ceramics with the thickness of 0.2 mm to investigate the relationship between the Ce^{3+} concentration and conversion ratio of blue light. As is shown in Fig. 2, the CIE color coordinates shift from the white-yellow region to yellow region as Ce concentration increases from 0.4 at % to 0.7 at %. The corresponding CCT decreases from 3315 K to 3080 K. Their fluorescent properties are also tabulated in table 1. Note that the increased Ce^{3+} concentration leads to a slightly red shift of spectrum, which can be observed from the photograph of ceramics (Fig. 2a). According to the luminescence performance of these CB-yLEDs, $(Ce_{0.6\%}Y_{69.4\%}Gd_{30\%})_3Al_5O_{12}$ ceramic is selected as the fluorescent matrix material.

3.2 Phase structures, microstructures and optical properties of (Ce,Gd):YAG-Al_2O_3 composite ceramics

Alumina has a thermal conductivity about three times that of YAG ceramics. In the present work, $(Ce_{0.6\%}Y_{69.4\%}Gd_{30\%})_3Al_5O_{12}$-z % Al_2O_3 (z = 0, 10, 20, 30, 40) composite ceramics were prepared and they were labeled as S0, S10, S20, S30, and S40, according to the corresponding component proportion of alumina. Their X-ray diffraction patterns are shown in Fig. 3. No intermediate phases ($YAlO_3$ or $Y_4Al_2O_9$) were detected in the sintered ceramics. The diffraction peaks of S0 match well with those of $Y_3Al_5O_{12}$ phase (JCPDS No. 79-1892). In the composite samples, the diffraction peaks of both YAG and Al_2O_3 phase (JCPDS No. 78-2426) can be observed and enhanced peak intensity of Al_2O_3 phase can be observed as the amount of Al_2O_3 increases.

Micrographs of five composite ceramics observed by SEM are shown in Fig. 4a~e. All samples exhibit dense polycrystalline structures and no pores are present. Darker grains appear in Fig. 4b~e and they are certified as Al_2O_3 grains, according to the

EDS mapping images of S20, as shown in Fig. 4f~j. When the proportion of Al_2O_3 increases from 10 wt% to 40 wt%, the average grain size of (Ce,Gd):YAG slightly decreases while that of Al_2O_3 increases from about 1 μm to 7 μm. The similar inhibitory effect on the growth of YAG grains has been observed in the previous literatures.[22, 23] Fine Al_2O_3 grains of S10 and S20 are uniformly embedded in the (Ce,Gd):YAG continuous phase. As the content of Al_2O_3 further increases, especially for S40, Al_2O_3 particles get bigger, denser and start to combine with each other and turn into quasi continuous phase. All samples show expected composite microstructures.

Fig. 5 shows the photographs of the composite ceramics. The (Ce,Gd):YAG transparent ceramic shows high light transmission and its in-line transmittance is over 65 % in the range of 500-780 nm. Two absorption peaks around 340 nm and 450 nm should be attributed to 4f → 5d transition of Ce^{3+} ions in YAG. Additional absorption peak located in 275 nm corresponds to the $^8S_{7/2} \rightarrow {}^6I_J$ transition of Gd^{3+} ions. Because of the difference between refractive index of (Ce,Gd):YAG and Al_2O_3 phase, the introduction of Al_2O_3 phase increases the scattering of light and the composite samples become translucent. The scattering behavior and extraction efficiency will be discussed in the subsequent sections.

3.3 Thermal quenching behavior and photoluminescent properties of composite ceramics

As the dominant commercial phosphor materials, Ce:YAG ceramics have excellent thermal behavior. As shown in Fig. 6c, the emission intensity of 0.6 at% Ce:YAG ceramics only decreases by 5 % when temperature increases from 25 °C to 200 °C. The thermal quenching effect originates from the aggravated non-radiative transition process at elevated temperature. When Gd^{3+} ions are doped in Ce:YAG ceramics for the purpose of the red shift of emission spectrum, the lower 5d energy level enables the excited electrons more easily undergo thermal activation to ground states. As a result, the emission intensity of $(Ce_{0.6\%}Y_{69.4\%}Gd_{30\%})_3Al_5O_{12}$ ceramic sample drops faster than that of Ce:YAG ceramics. The better thermal stability of Al_2O_3-based composite ceramics has been reported in previous literatures. [18, 22] In this work, the thermal quenching behavior of composite ceramics gets only slightly alleviated, as shown in Fig. 6b~c. It may be due to the negligible impact of Al_2O_3 phase on the energy level structure of Ce^{3+} ions in (Ce,Gd):YAG. The corresponding luminescence lifetimes of composite ceramics were measured. All samples exhibit single-exponential decay of about 66-69 ns, thus confirming that the fluorescent environment has not obvious change as a function of Al_2O_3 amount.

It can also be found in the fig. 6c that the luminescent properties of Gd^{3+} doped samples are quite sensitive to temperature. We can utilize the improvement of thermal conductivity of composite ceramics to indirectly improve the thermal behavior of (Ce,Gd):YAG by decreasing the temperature of ceramics at runtime. As expected, thermal conductivity increases from 7.244 W m^{-1} K^{-1} to 13.944 W m^{-1} K^{-1} when the content of Al_2O_3 increases from 10 wt% to 40 wt% (Fig. 7a). The effect of improved

thermal conductivity on the operating temperature of CB-yLEDs was studied. As shown in Fig. 8, InGaN/GaN LED chips were mounted on AlN substrate and the composite ceramics with the thickness of 0.20 mm were cut into square slice, and then packaged on these chips. The forward current was fixed at 1.3 A. The real-time temperature of composite ceramics (T_c) and substrate (T_s) were monitored by thermal imaging camera. As shown in Fig. 7b~f, both T_c and temperature difference (ΔT) between T_c and T_s gradually decreases as the content of Al_2O_3 increases. The time dependence of T_c and ΔT of these CB-yLEDs are plotted in Fig. 9. Attributed to the increased thermal conductivity, CB-yLEDs with high amount of Al_2O_3 conduct heat faster. ΔT gradually decreases from 17.3 °C to 10.9 °C as the amount of Al_2O_3 increases from 0 wt% to 40 wt%, which means that Al_2O_3-free CB-yLEDs have higher operating temperature in the same condition than composite samples. Moreover, the higher temperature further decreases quantum efficiency of CB-yLEDs and generates more heat. Based on these factors, steady-state temperature of CB-yLEDs decreases from 141.1 °C to 132.2 °C as the amount of Al_2O_3 increases. Significantly, as shown in Fig. 6b, temperature of ceramics has a great influence on the luminescent properties.

We use the integrated optical and electrical measuring system (Fig. 8c) to monitor luminous efficiency (LE) of these CB-yLEDs (Fig. 10). When the CB-yLEDs light up, the transient LEs of all samples are quite close and the highest transient LE reaches 131.01 lm/W, benefiting from the relative low temperature of ceramics. As the running time increases, LEs of all samples decreases rapidly and gradually maintain stability after 10 minutes, the trends of which are well corresponding to that of operating temperature. The steady-state LE of S0 sample decreases to 100.88 lm/W, which is 21.35 % lower than the initial LE. As the content of Al_2O_3 increases, the steady-state LE monotonically increases and the LE of S40 sample reaches the highest value of 109.49 lm/W, which is 8.54 % higher than that of S0 sample. The results show that the introduction of Al_2O_3 phase can effectively improve the thermal and luminescent properties of CB-yLEDs.

3.4 Scattering behavior and conversion efficiency of CB-yLEDs

One additional consideration for CB-yLEDs is their scattering behavior and extraction efficiency. Al_2O_3 phase can introduce scattering, resulting in altered light propagation and enhanced extraction efficiency. However, the introduction of Al_2O_3 phase also reduces the amount of Ce^{3+} ions in ceramics (Fig. 11f). Compared with S0 sample, the amount of Ce^{3+} ions in S40 sample reduces by about 45 %. Both of the two factors influence the conversion efficiency of blue light. Excited by 450 nm blue light, the emission spectra of five composite ceramics are plotted in Fig. 11a~e. The thickness of ceramics is introduced as an additional parameter because the path of light propagation is related to the thickness of composite ceramics. The integrated emission intensity is normalized by setting those of S0 samples to 100%. When the thickness of ceramics is 1.0 mm, the effect of light scattering by Al_2O_3 phase dominates and the composite ceramics exhibit excellent light conversion and extraction efficiency. Especially for S40 sample, it has the highest integrated emission intensity, which is

about 3.25 times that of (Ce,Gd):YAG ceramics.

However, as the thickness of composite ceramics decreases to 0.6 mm and 0.4 mm, the effect of scattering of Al_2O_3 phase gets weakened and the relative emission intensity of composite samples decreases but is still higher than that of S0 sample. The two factors mentioned above reach a relative balance when the thickness of ceramics decreases to 0.2 mm. Emission intensity of all samples remains largely the same, besides a slight decrease of emission intensity when the content of Al_2O_3 phase reaches 40 wt%.

The spectra of CB-yLEDs encapsulated by 0.2 mm-thickness composite ceramics are shown in Fig. 12a~b. Their luminescent properties are tabulated in table 2. Besides S40, there is little difference in the intensity of unconverted blue light, which further strengthens the evidence of light conversion behavior described in Fig. 11. When the content of Al_2O_3 phase is below 30 wt%, the distribution of color coordinates and CCT is centralized. Attributed to the higher proportion of blue light in the spectrum of S40, the corresponding color coordinates gets shift to white-yellow region and the CCT increases to 3437 K. Another notable phenomenon is that a slight blue-shifted emission (≈ 3 nm) can be observed as the amount of Al_2O_3 increases. This kind of blue shift has been reported by Song *et al*. and the possible reason is that the addition of Al_2O_3 mitigates the effect of reabsorption of the scattered blue light.[19, 24]

4. Conclusion

The realization of phosphor ceramics is required for the high-brightness yellow LED (565-590 nm) due to its high thermal conductivity than resins and glasses. In the 0.2 mm-thickness YAG ceramics, 30 at% Gd^{3+} ions were doped for the spectral modulation of yLEDs. However, the introduction of Gd^{3+} ions exacerbated the thermal quenching effect. To conduct heat faster at high temperature, Al_2O_3 phase (32-35 W m^{-1} K^{-1}) was introduced and $(Ce_{0.6\%}Y_{69.4\%}Gd_{30\%})_3Al_5O_{12}$-z% Al_2O_3 (z=0, 10, 20, 30, 40) composite ceramics were prepared. All samples show expected composite microstructures and no reactivity between Al_2O_3 and (Ce,Gd):YAG phase. As the proportion of Al_2O_3 phase increases from 0 wt% to 40 wt%, thermal conductivity of composite ceramics increases from 7.244 W m^{-1} K^{-1} to 13.944 W m^{-1} K^{-1}. Consequently, temperature difference (ΔT) between ceramics (T_c) and substrate (T_s) gradually decreases from 17.3 °C to 10.9 °C and the steady-state temperature of ceramic-based yellow LEDs (CB-yLEDs) decreases from 141.1 °C to 132.2 °C. Meanwhile, the thermal stability of composite ceramics increases by the introduction of Al_2O_3 phase. Based on these advantages, the steady-state luminous efficiency (LE) of S40 sample reaches the highest value of 109.49 lm/W, which is 8.54 % higher than that of S0 sample. Excellent light scattering behavior combined with the reduced Ce^{3+} amount, all 0.2 mm-thickness Al_2O_3-based composite ceramics exhibits similar conversion efficiency of blue light, except for S40 sample with more unconverted blue light because of the deficiency of Ce^{3+} amount.

Declaration of Competing Interest

The authors report no declarations of interest.

Acknowledgements

This work was supported by Fujian Science & Technology Innovation Laboratory for Optoelectronic Information of China (No. 2021ZZ113 and No. 2021ZR103) and the Youth Science Funds of Fujian Province (No. 2019J05153).

References

[1] Pust P, Schmidt P J, Schnick W. A revolution in lighting. *Nat Mater* 2015,**14**(5):454-458.

[2] Haitz R, Tsao JY. Solid-state lighting: 'The case' 10 years after and future prospects, *physica status solidi (a).*2011, **208**(1);17-29.

[3] Yao HW, Mueller-Mach R, Mueller GO, *et al*. White-light-emitting diodes for illumination. *Proceedings of SPIE*, 2000:30-41.

[4] Pattison PM, Tsao JY, Brainard GC, *et al*. LEDs for photons, physiology and food, *Nature.*2018, **563**(7732): 493-500.

[5] Pattison M, Hansen M, Bardsley N, *et al*. DOE BTO Lighting R&D Program, "2019 Lighting R&D Opportunities" 2019.

[6] Pattison PM, Hansen M, Tsao JY. LED lighting efficacy: Status and directions, *Cr Phys*. 2018,**19**(3) :134-145.

[7] Xia ZG, Xu ZH, Chen MY, *et al.* Recent developments in the new inorganic solid-state LED phosphors, *Dalton T*. 2016, **45**(28):11214-11232.

[8] Ye S, Xiao F, Pan YX, *et al*. Phosphors in phosphor-converted white light-emitting diodes: Recent advances in materials, techniques and properties. *Mat Sci Eng R.* 2010, **71**(1):1-34.

[9] Nishiura S, Tanabe S, Fujioka K, *et al*. Properties of transparent Ce:YAG ceramic phosphors for white LED. *Opt Mater.* 2011, **33**(5):688-691.

[10] Yao Q, Hu P, Sun P, *et al*. YAGCe^{3+} Transparent Ceramic Phosphors Brighten the Next-Generation Laser-Driven Lighting, *Adv Mater* 2020, **1907888**.

[11] Chen L, Chen X, Liu F, *et al.* Charge deformation and orbital hybridization: intrinsic mechanisms on tunable chromaticity of $Y_3Al_5O_{12}$:Ce^{3+} luminescence by doping Gd3+ for warm white LEDs, *Sci Rep* 2015,**5**:11514.

[12] Hu C, Shi Y, Feng X, *et al.* YAG:Ce/(Gd,Y)AG:Ce dual-layered composite structure ceramic phosphors designed for bright white light-emitting diodes with various CCT, *Opt Express*. 2015, **23**(14) 18243-18255.

[13] Chen J, Deng ZH, Liu ZG, *et al.* Optical enhancement brought by doping Gd(3+) ions into Ce: YAG ceramics for indoor white light-emitting diodes, *Opt Express* 2015, **23**(7): A292-298.

[14] Liu X, Qian X, Hu Z, *et al.* Al_2O_3-Ce:GdYAG composite ceramic phosphors for high-power white light-emitting-diode applications. *J Eur Ceram Soc.* 2019, **39**(6):2149-2154.

[15] Su LT, Tok AIY, Zhao Y, *et al*. Synthesis and Electron-Phonon Interactions of Ce^{3+}-Doped YAG Nanoparticles, *J Phys Chem C* 2009, **113**(15):5974-5979.

[16] Wen B, Zhang DF, Jiang B,*et al.* Thermal conductivity of Ce^{3+} doped (Y,Gd)(3)Al5O12 ceramic

phosphor, *J Lumin*. 2020, **221**.

[17] Li S, Zhu Q, Tang D, *et al.* Al_2O_3–YAG:Ce composite phosphor ceramic: a thermally robust and efficient color converter for solid state laser lighting. J Mater Chem C. 2016, **4**(37) :8648-8654.

[18] Wang J, Tang X, Zheng P, *et al.* Thermally self-managing YAG_Ce-Al_2O_3 color converters enabling high-brightness laser-driven solid state lighting in a transmissive configuration, *J. Mater. Chem. C*. 2019, **7**:3901-3908.

[19] Cozzan C, Lheureux G, O'Dea N, *et al*. Stable, Heat-Conducting Phosphor Composites for High-Power Laser Lighting, *Acs Appl Mater Inter.* 2018, **10**(6): 5673-5681.

[20] Zheng P, Li SX, Wei R, *et al*. Unique Design Strategy for Laser-Driven Color Converters Enabling Superhigh-Luminance and High-Directionality White Light. *Laser Photonics Rev.* 2019 **13**(10).

[21] Li XY, Chen J, Liu ZG, *et al.* Effect of air annealing on the optical properties and luminescence performance of Ce:YAG ceramics for light-emitting diodes at different Ce concentrations. *J Eur Ceram Soc.* 2021, **41**(8):4590-4597.

[22] Hu S, Zhang YL, Wang ZJ, *et al*. Phase composition, microstructure and luminescent property evolutions in "light-scattering enhanced" Al_2O_3-$Y_3Al_5O_{12}$: Ce^{3+} ceramic phosphors, *J Eur Ceram Soc.* 2018, **38**(9):3268-3278.

[23] Yang H, Qin XP, Zhang J, *et al*. Fabrication of Nd:YAG transparent ceramics with both TEOS and MgO additives. *J Alloy Compd.* 2011, **509**(17):5274-5279.

[24] Song YH, Ji EK, Jeong BW, *et al*. Design of laser-driven high-efficiency Al_2O_3/YAG:Ce^{3+} ceramic converter for automotive lighting: Fabrication, luminous emittance, and tunable color space. *Dyes Pigments.* 2017, **139**: 688-692.

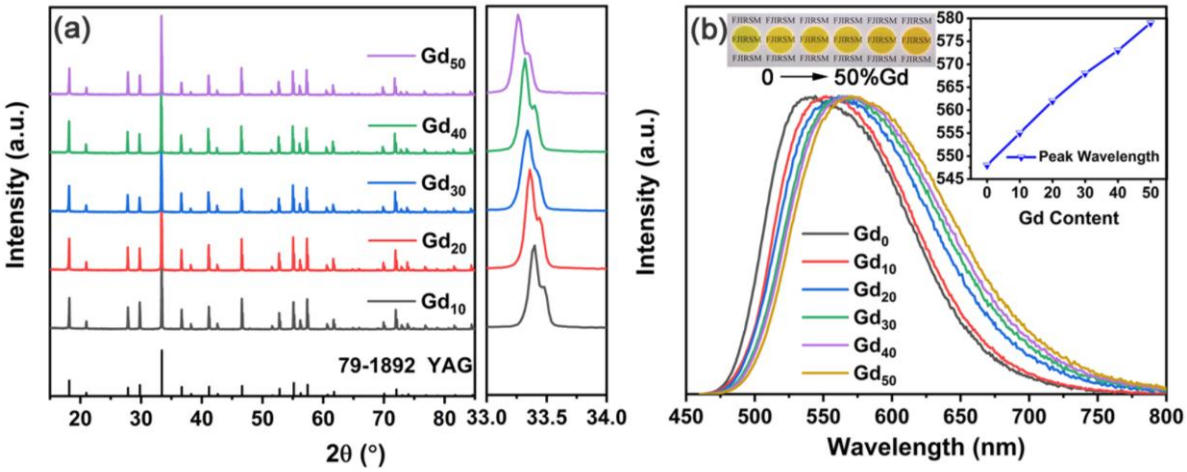

Fig. 1 (a) XRD patterns and (b) the normalized photoluminescence spectra of $(Ce_{0.6\%}Y_{99.4\%-x\%}Gd_{x\%})_3Al_5O_{12}$ (x=0, 10, 20, 30, 40, 50) transparent ceramics.

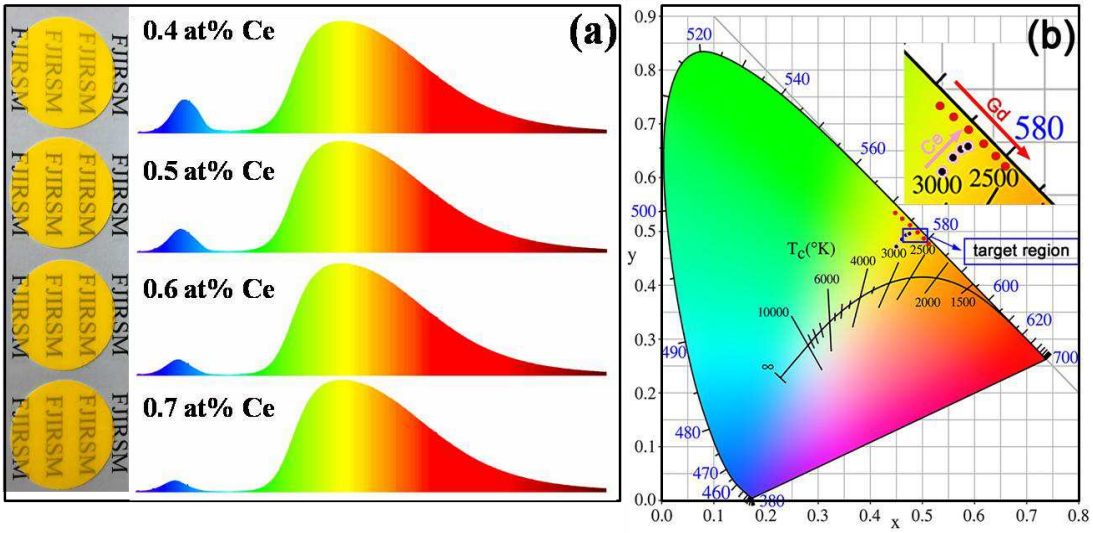

Fig. 2 (a) Images, measured electroluminescent spectra and (b) CIE coordinates of 0.2 mm-thickness $(Ce_{y\%}Y_{70\%-y\%}Gd_{30\%})_3Al_5O_{12}$ (y=0.4, 0.5, 0.6, 0.7) transparent ceramics.

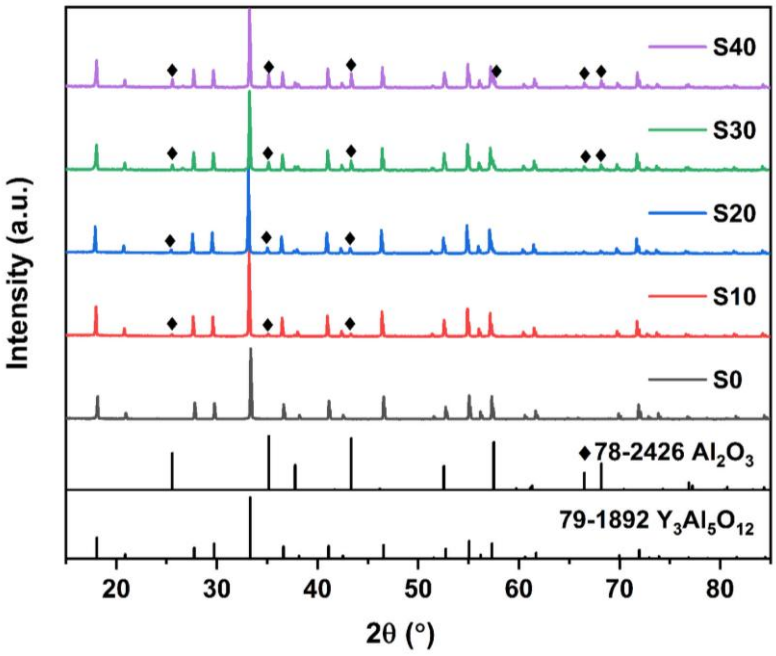

Fig.3 XRD patterns of $(Ce_{0.6\%}Y_{69.4\%}Gd_{30\%})_3Al_5O_{12}$-z % Al_2O_3 (z = 0, 10, 20, 30, 40) composite ceramics.

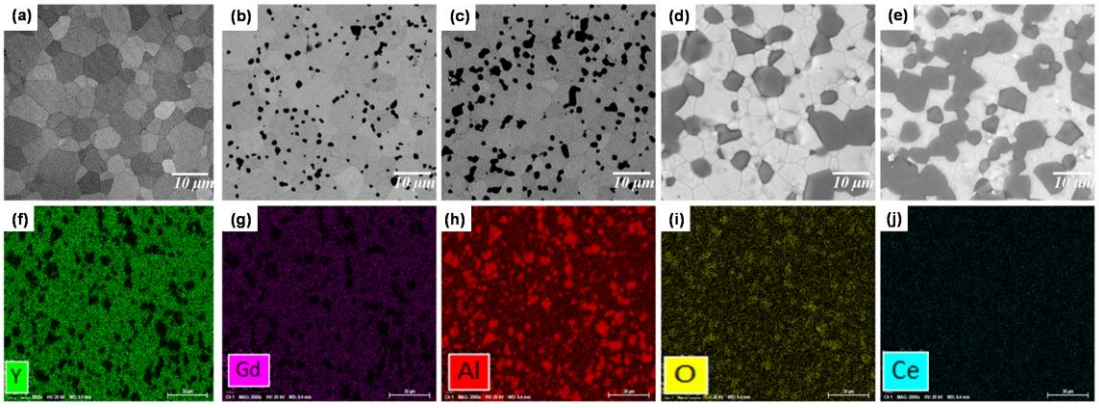

Fig.4 FE-SEM images of (Ce,Gd):YAG-Al_2O_3 composite ceramics with (a) 0 wt%, (b) 10 wt%, (c) 20 wt%, (d) 30 wt%, (e) 40 wt% Al_2O_3 concentrations and EDS mapping images of (f) Y element, (g) Gd element, (h) Al element, (i) O element and (j) Ce element of S20 sample.

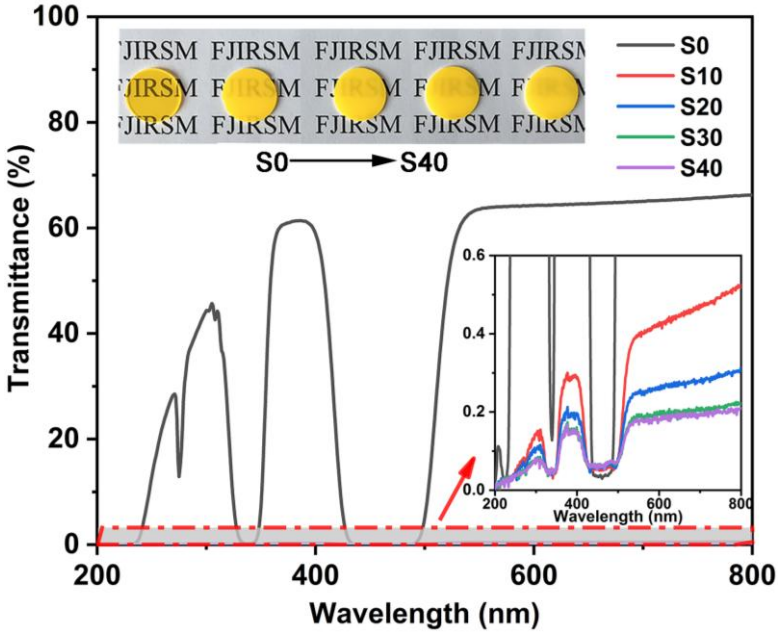

Fig.5 Images and in-line transmittance of (Ce,Gd):YAG-Al_2O_3 composite ceramics.

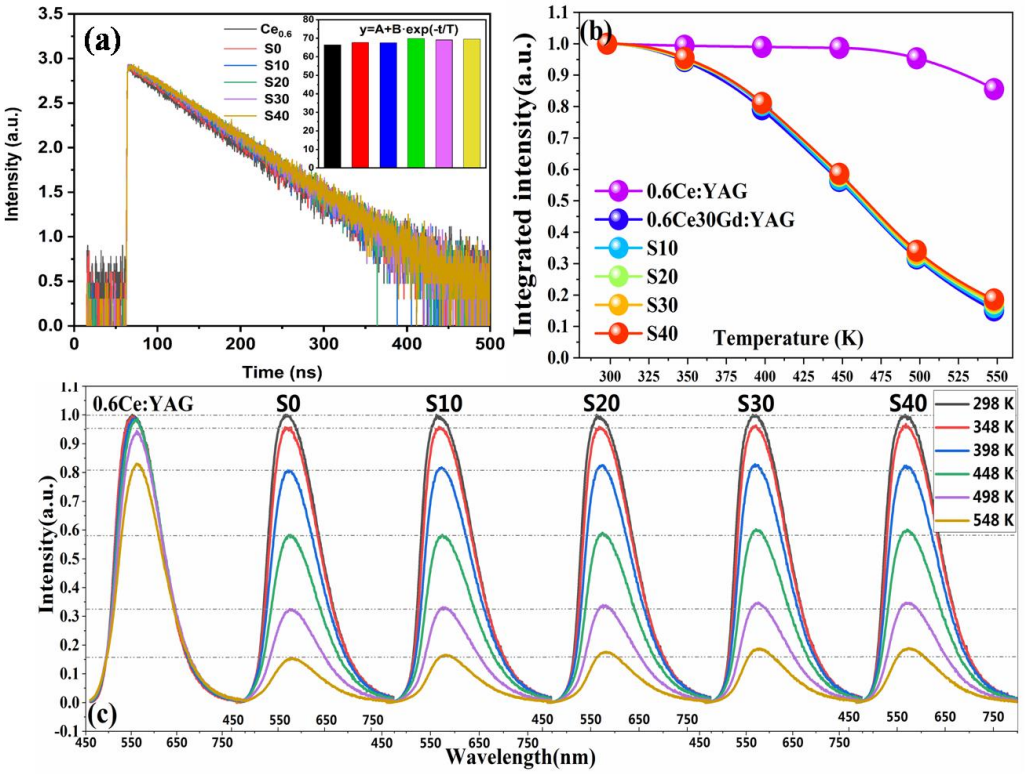

Fig.6 (a) Measured fluorescence lifetime and (b) the temperature-dependent integrated emission intensity of (Ce,Gd):YAG-Al_2O_3 composite ceramics with different Al_2O_3 contents; (c) the corresponding normalized emission intensity of all composite samples.

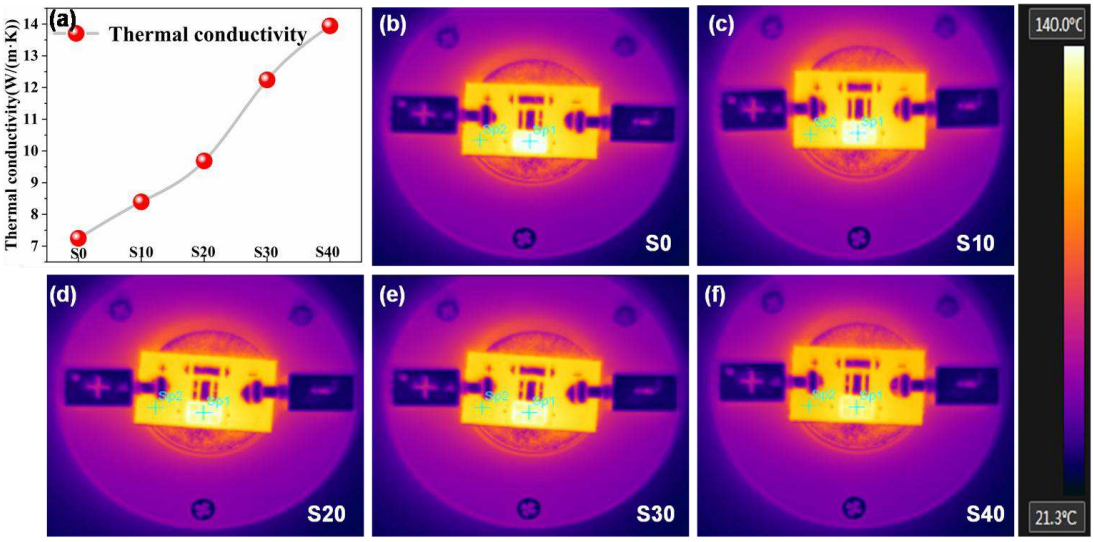

Fig.7 (a) Thermal conductivity as a function of Al_2O_3 content at room temperature; (b) ~ (f) monitored images of real-time temperature of composite ceramics (Tc) and substrate (Ts) by thermal imaging camera.

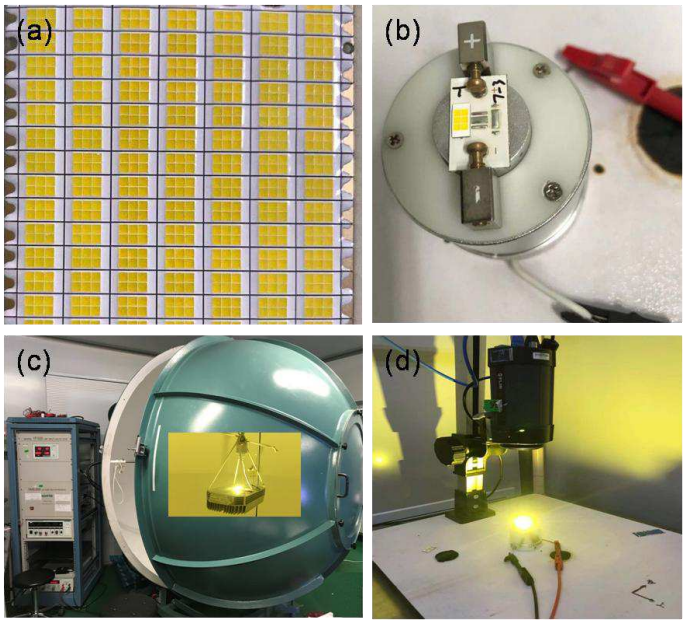

Fig.8 Images of (a) ~ (b) yellow LEDs encapsulated by composite ceramics; (c) the integrated optical and electrical measuring system; (d) operating CB-yLEDs monitored by thermal imaging camera.

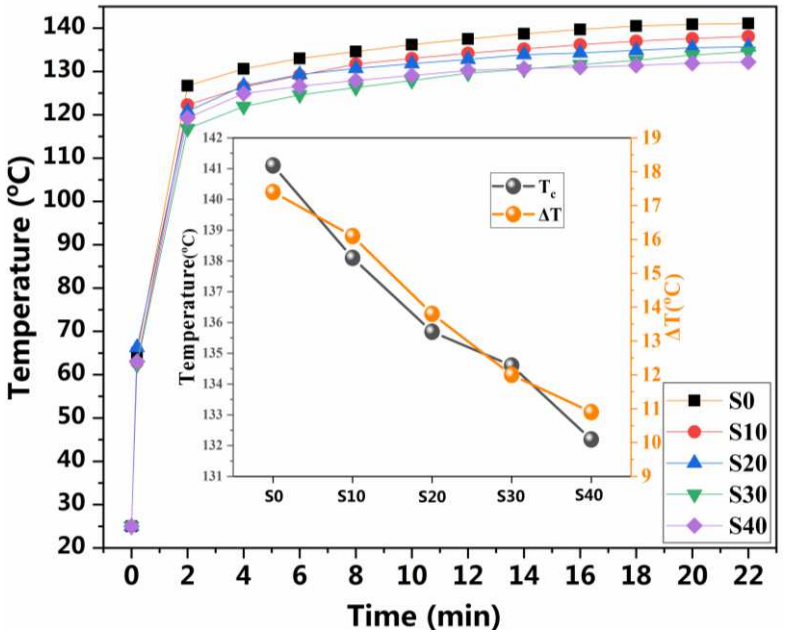

Fig.9 The time-dependent temperature of composite ceramics (T_c) and temperature difference (ΔT) between T_c and T_s as a function of Al_2O_3 content.

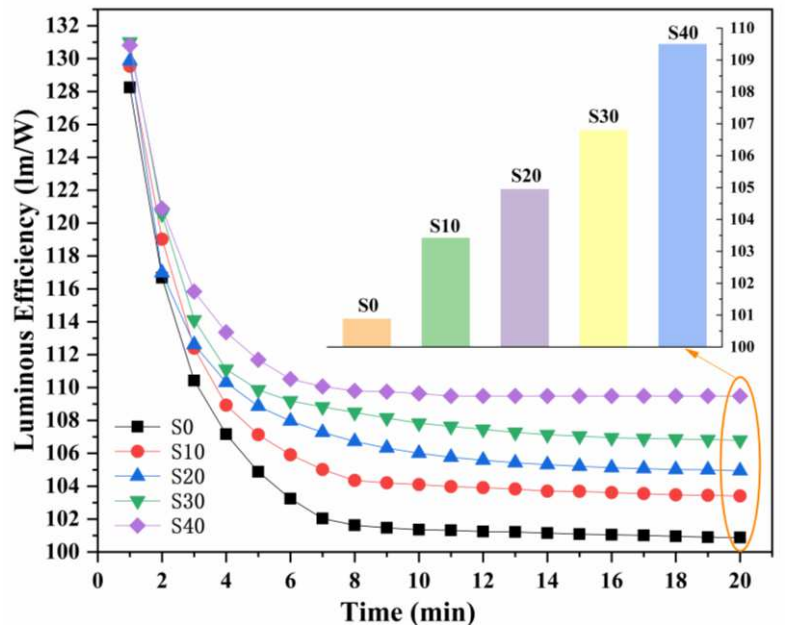

Fig.10 The time-dependent luminous efficiency (LE) of CB-yLEDs as a function of Al_2O_3 content (The forward current was fixed at 1.3 A).

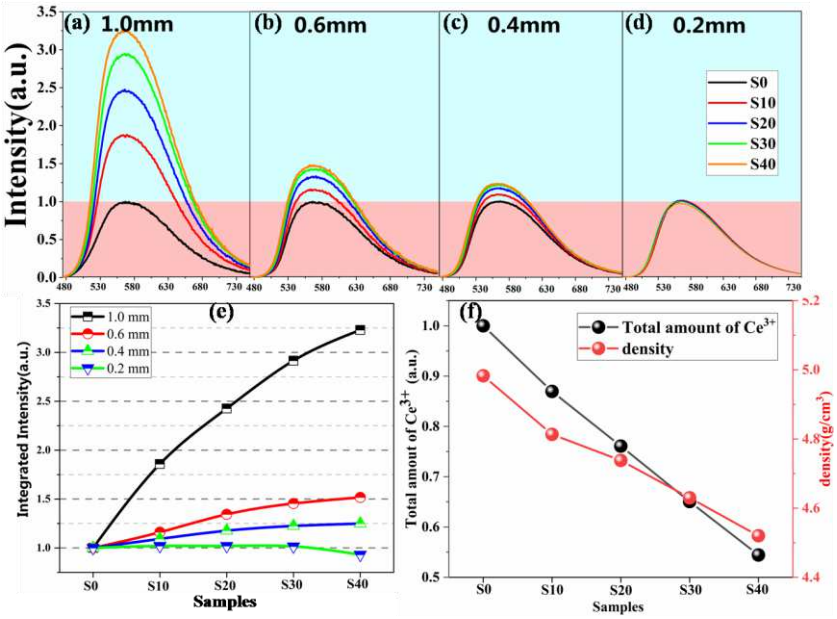

Fig.11 Normalized emission spectra of five composite ceramics with the thickness of (a) 1.0 mm, (b) 0.6 mm, (c) 0.4 mm, (d) 0.2 mm and (e) their integrated emission intensities; (f) density and relative amount of Ce^{3+} ions as a function of Al_2O_3 content.

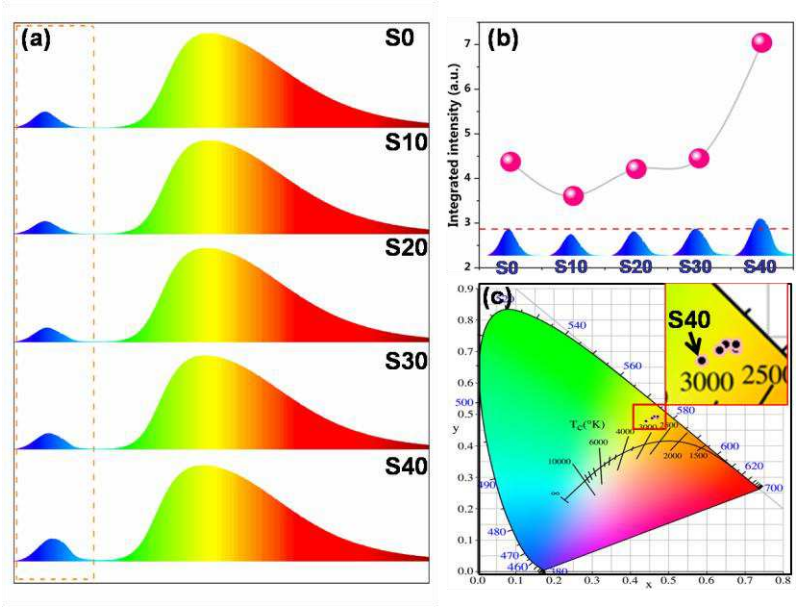

Fig.12 (a) Measured electroluminescent spectra of five Al_2O_3-based CB-yLEDs; (b) integrated intensities of unconverted blue light as a function of Al_2O_3 content; (c) corresponding CIE coordinates.

Table 1 Measured luminescent properties of $(Ce_{0.6\%}Y_{99.4\%-x\%}Gd_{x\%})_3Al_5O_{12}$ (x=0, 10, 20, 30, 40, 50) and $(Ce_{y\%}Y_{70\%-y\%}Gd_{30\%})_3Al_5O_{12}$ (y=0.4, 0.5, 0.6, 0.7) ceramics-based yellow LEDs.

Samples	Thickness (mm)	Emission peak (nm)	CCT (K）	CIE (x, y)
0.6%CeYAG:0%Gd	1.0	548	3655	(0.4476,0.5349)
0.6%CeYAG:10%Gd	1.0	555	3405	(0.4618,0.5243)
0.6%CeYAG:20%Gd	1.0	562	3146	(0.4759,0.5120)
0.6%CeYAG:30%Gd	1.0	568	2879	(0.4902,0.4990)
0.6%CeYAG:40%Gd	1.0	573	2699	(0.5030,0.4864)
0.6%CeYAG:50%Gd	1.0	579	2540	(0.5115,0.4769)
30%GdYAG:0.4%Ce	0.2	566	3315	(0.4503,0.4720)
30%GdYAG:0.5%Ce	0.2	566	3208	(0.4607,0.4854)
30%GdYAG:0.6%Ce	0.2	568	3107	(0.4708,0.4899)
30%GdYAG:0.7%Ce	0.2	569	3080	(0.4757,0.4958)

Table 2 Measured luminescent properties of $(Ce_{0.6\%}Y_{69.4\%}Gd_{30\%})_3Al_5O_{12}$-z % Al_2O_3 (z = 0, 10, 20, 30, 40) composite ceramics-based yellow LEDs.

Samples	Emission peak (nm)	LF(lm)	LE (lm/W)	CCT (K)	CIE (x, y)
S0	568	1138.74	100.88	3107	(0.4708,0.4899)
S10	568	1162.26	103.41	3114	(0.4714,0.4935)
S20	567	1186.39	104.94	3220	(0.4630,0.4928)
S30	566	1205.06	106.80	3268	(0.4577,0.4883)
S40	565	1237.98	109.49	3437	(0.4438,0.4828)